Hysteresis regime in the operation of a dual-free-layer spin-torque nano-oscillator with out-of-plane counter-precessing magnetic moments

O. V. Prokopenko*
Faculty of Radiophysics, Taras Shevchenko National University of Kyiv, Kyiv 01601, Ukraine

I. N. Krivorotov
Department of Physics and Astronomy, University of California, Irvine, CA 92697, USA

E. N. Bankowski and T. J. Meitzler
Department of Ground Systems Survivability, U.S. Army TARDEC, Warren, MI 48397, USA

V. S. Tiberkevich and A. N. Slavin
Department of Physics, Oakland University, Rochester, MI 48309, USA
(Dated: July 21, 2013)

The operation of a dual-free-layer (DFL) spin-torque nano-oscillator (STNO) is studied is demonstrated that in a practically interesting regime when the magnetizations of the two free layers (FLs) precess in opposite directions along large-angle out-of-plane trajectories, thus doubling the generation frequency, the operation of the DFL STNO is strongly hysteretic as a function of a bias dc current. The stable magnetization dynamics starts at a rather large magnitude of the bias dc current density $J_{\rm dc} > J_{\rm th}^{\rm high}$ when the bias current is increased, but the regime of stable counter-precession of the FLs persists till rather low magnitudes of the bias dc current density $J_{\rm th}^{\rm low} < J_{\rm dc} < J_{\rm th}^{\rm high}$ when the bias current is decreased. This hysteresis is caused by the dipolar coupling between the FLs, and is especially pronounced for small distances between the FLs and small magnetic damping in them. The discovered hysteretic behavior of the DFL STNO implies the possibility of application of a strong initial pulse of the bias current (greater than the upper threshold $J_{\rm th}^{\rm high}$ of the stable dynamics) and subsequent reduction of the bias current to a working point ($J_{\rm th}^{\rm low} < J_{\rm dc} < J_{\rm th}^{\rm high}$) corresponding to the required output frequency $f(J_{\rm dc})$. The obtained results might be important for the practical development of DFL STNOs with optimized operation characteristics.

PACS numbers: 85.75.-d, 07.57.Hm, 84.40.-x

I. INTRODUCTION

The spin-transfer torque (STT) effect [1–4] in magnetic multilayers theoretically predicted by L. Berger and J. C. Slonczewski provides a new method of manipulation of the magnetization dynamics in nano-magnetic systems [5, 6]. The spin-torque nano-oscillators (STNOs), based on the STT effect, are now considered as promising base elements for various nano-scale microwave devices, particularly, microwave signal sources [7–17] and microwave detectors [18–25]. However, for these devices to become practical in modern microwave signal processing systems it is necessary to enlarge the range of their operational frequencies, to improve their phase noise characteristics, and to increase their integrated output power [26, 27]. It is, also, preferable that these devices should be able to operate in a zero (or very low) bias dc magnetic field.

A step towards the development of such a practical STNO has been made in [28], where an oscillator with a perpendicular polarizer has been suggested and demonstrated experimentally. In the STNO proposed in [28] the free magnetic layer (FL) was situated between the perpendicular polarizer and an in-plane magnetized reference layer. The magnetization of the free layer was pushed out of plane by STT from the polarizer and at a sufficiently large bias current it was precessing along a large amplitude trajectory around the resulting easy-plane shape anisotropy field [29, 30]. The stationary precession of the FL magnetization with respect to the static perpendicular magnetization of the reference layer results in the microwave-frequency oscillations of the device resistance transformed in a microwave voltage signal by means of the giant magneto-resistance (GMR) effect between the layers [28]. Because of the relatively large oscillation amplitude this type of STNO offers a significant improvement in microwave power emission over conventional STNOs consisting of an in-plane FL and an in-plane pinned magnetic layer (PL). The main limitation of this structure, however, is a relatively low maximum frequency caused by the formation of a static vortex in the FL at high densities of the dc current [29].

In this paper, we consider a symmetric dual-free-layer (DFL) STNO, containing two perpendicularly polarized PLs and two adjacent FLs with easy-plane anisotropy (Fig. 1(a)). It has been suggested recently that such a DFL STNO could be used as a high-frequency microwave source in zero bias magnetic field, because in such a geometry it is possible to achieve the opposite di-

*Electronic address: ovp@univ.kiev.ua

Report Documentation Page

Form Approved
OMB No. 0704-0188

1. REPORT DATE	2. REPORT TYPE	3. DATES COVERED
01 AUG 2013	**Journal Articles**	**07-03-2013 to 12-07-2013**

4. TITLE AND SUBTITLE
Hysteresis regime in the operation of a dual-free-layer spin-torque nano-oscillator with out-of-plane counter-precessing magnetic moments

5a. CONTRACT NUMBER
ECCS-1001815, ECCS-1002358, DMR-101

5b. GRANT NUMBER

5c. PROGRAM ELEMENT NUMBER

6. AUTHOR(S)
O Prokopenk; I Krivorotov; T Meitzler; E Bankowski; V Tiberkevich

5d. PROJECT NUMBER

5e. TASK NUMBER

5f. WORK UNIT NUMBER

7. PERFORMING ORGANIZATION NAME(S) AND ADDRESS(ES)
Department of Physics and Astronomy,University of California,405 Hilgard Ave,Irvine,CA,92697

8. PERFORMING ORGANIZATION REPORT NUMBER
; #24043

9. SPONSORING/MONITORING AGENCY NAME(S) AND ADDRESS(ES)
U.S. Army TARDEC, 6501 East Eleven Mile Rd, Warren, Mi, 48397-5000

10. SPONSOR/MONITOR'S ACRONYM(S)
TARDEC

11. SPONSOR/MONITOR'S REPORT NUMBER(S)
#24043

12. DISTRIBUTION/AVAILABILITY STATEMENT
Approved for public release; distribution unlimited

13. SUPPLEMENTARY NOTES
Submitted to IEEE Magnetic Letters Journal

14. ABSTRACT

The operation of a dual-free-layer (DFL) spin-torque nano-oscillator (STNO) is studied is demonstrated that in a practically interesting regime when the magnetizations of the two free layers (FLs) precess in opposite directions along large-angle out-of-plane trajectories, thus doubling the generation frequency, the operation of the DFL STNO is strongly hysteretic as a function of a bias dc current. The stable magnetization dynamics starts at a rather large magnitude of the bias dc current density Jdc > Jhigh th when the bias current is increased, but the regime of stable counter-precession of the FLs persists till rather low magnitudes of the bias dc current density Jlow th < Jdc < Jhigh th when the bias current is decreased. This hysteresis is caused by the dipolar coupling between the FLs, and is especially pronounced for small distances between the FLs and small magnetic damping in them. The discovered hysteretic behavior of the DFL STNO implies the possibility of application of a strong initial pulse of the bias current (greater than the upper threshold Jhigh th of the stable dynamics) and subsequent reduction of the bias current to a working point (Jlow th < Jdc < Jhigh th) corresponding to the required output frequency f(Jdc). The obtained results might be important for the practical development of DFL STNOs with optimized operation characteristics.

15. SUBJECT TERMS

16. SECURITY CLASSIFICATION OF:			17. LIMITATION OF ABSTRACT	18. NUMBER OF PAGES	19a. NAME OF RESPONSIBLE PERSON
a. REPORT **unclassified**	b. ABSTRACT **unclassified**	c. THIS PAGE **unclassified**	**Public Release**	**10**	

Standard Form 298 (Rev. 8-98)
Prescribed by ANSI Std Z39-18

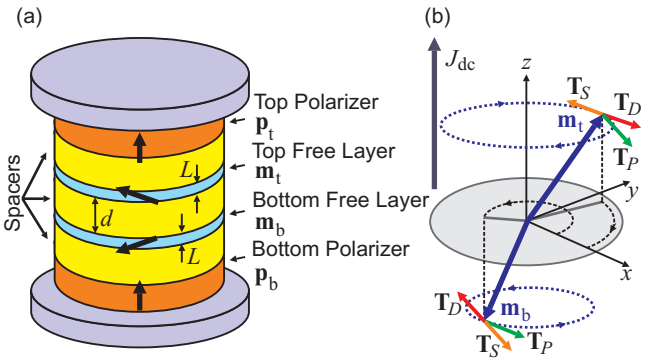

FIG. 1: (Color Online) (a) Layout of the symmetric dual-free-layer (DFL) STNO consisting of four magnetic layers: two inner free magnetic layers (FLs) of the thickness L and two outer pinned layers with perpendicular polarization separated by the GMR spacer of the thickness d. (b) The torques acting on the magnetization vectors of the FLs in the DFL STNO driven by the transverse bias dc current of the density J_{dc}. The conservative torque ($\mathbf{T}_P$) caused by the effective magnetic field $\mathbf{B}_{eff}$ induces magnetization precession in the FLs around the normal to the STNO layers. The non-conservative spin-torques ($\mathbf{T}_S$) caused by the perpendicular polarizers adjacent to each of the FLs tend to increase the precession angle, while the non-conservative torques ($\mathbf{T}_D$) caused to the Gilbert damping in the FLs tend to reduce it.

rections of the current-driven magnetization precession in the FLs, and, therefore, to double the generated microwave frequency (the angle between the magnetizations of the FLs in a DFL DTNO changes twice as fast as the angle between the magnetizations of the free and pinned layers) [31]. Below we consider the regime of a DFL STNO operation, when the FL magnetizations precess *in the opposite directions* along the large-angle out-of-plane (OOP) trajectories and generate a relatively large microwave power at a frequency that is a sum of the magnetization precession frequencies in individual FLs.

Although the physical mechanism of the frequency doubling in the proposed regime of the DFL STNO operation seems to be simple and obvious, it is not unique. It has been shown in [32] that the frequency doubling in a DFL STNO structure can be also achieved when the magnetizations of the FLs precess in the same direction, but are phase-shifted. In our theoretical considerations below we will not explicitly consider this "phase-shifted" case. Recent micromagnetic simulations performed in [33] have shown that the regime of the DFL STNO operation with counter-precessing FLs is limited by a rather high dc current density threshold J_{th} needed for the excitation of a stable OOP precession in the FLs ($J_{dc} > J_{th}$) and by the formation of a vortex in the FL at higher dc current densities ($J_{dc} > J_{vortex}$). It is important to note, that the dc current density threshold J_{th} found from the micromagnetic simulations is of the order of $J_{th} \approx 0.35 \cdot 10^8$ A/cm^2 for a DFL STNO with typical parameters [33] and substationally exceeds the threshold for a conventional single-free-layer STNO with similar parameters. Consequently, the range of the DFL STNO operation frequencies in the regime with counter-precessing FLs ($\sim J_{vortex}/J_{th}$) is smaller than the similar range for a conventional single-free-layer STNO. This limited frequency range complicates the practical applications of the DFL STNO for microwave signal generation, while a rather high dc current density threshold J_{th} limits the reliability of such devices.

In this work, using a simple numerical macrospin model described in Section II, we study the operation of a DFL STNO in the regime with counter-precessing FLs in a wide range of bias dc current densities J_{dc} and reveal the existence of a strong hysteresis in the dependence of the operational parameters of a DFL STNO on the bias current density. In the Section III we show that a stable counter-precession of magnetizations of the FLs, indeed, starts at a rather large magnitude of the bias current density $J_{dc} = J_{th}^{high}$ (approximately equal to the bias dc current density threshold J_{th} found from the micromagnetic simulations [33]) when the bias current density is increased. However, the regime of stable counter-precession persists till rather low magnitudes of the bias current $J_{dc} = J_{th}^{low}$ when the bias current density is decreased. We demonstrate that the lower threshold J_{th}^{low} is mainly determined by the damping in the system (like the threshold in a conventional single-free-layer STNO), while the upper threshold J_{th}^{high} of the auto-oscillation regime is mainly determined by the existence of a dipolar coupling between the FLs and/or by the in-plane anisotropy in the FLs.

Therefore, a relatively large external bias current is needed only *to start the auto-oscillations* in the device, and after the auto-oscillations have started it is possible to significantly reduce the bias current density to J_{th}^{low} while preserving the regime of stable counter-precessing magnetizations of the FLs of the device at a working point ($J_{th}^{low} < J_{dc} < J_{th}^{high}$) corresponding to the required output frequency $f(J_{dc})$. We believe that the obtained results might be important for the practical development of DFL STNOs with optimized working characteristics.

II. MODEL

A. Schematic and fundamentals of the DFL STNO

The layout of a symmetric DFL STNO is shown in Fig. 1(a). The STNO is a circular nano-pillar consisting of four metallic ferromagnetic layers separated by three non-magnetic spacers. The outermost magnetic layers serve as current polarizers, and are composed of the materials with perpendicular magnetic anisotropy that is sufficiently large to keep the magnetizations of these layers out of the sample plane along the z-axis of the coordinate system shown in Fig. 1(b) ($\mathbf{p}_i = \hat{\mathbf{z}}$ are the unit vectors in the direction of the magnetizations of the polarizers, $i = $ t and $i = $ b for the top and bottom layers, respectively, $\hat{\mathbf{z}}$ is the unit vector of the z-axis).

The magnetizations $\mathbf{M}_i$ of the two inner ferromagnetic layers lie in the plane of the sample at equilibrium, and these layers serve as the FLs of the STNO ($\mathbf{M}_i = M_{f,\,i}\,\mathbf{m}_i$, $M_{f,\,i}$ is the saturation magnetization of the ith FL, $\mathbf{m}_i$ is the unit vector along the magnetization vector in the ith FL, $i = \{\mathrm{t},\,\mathrm{b}\}$).

In the presence of a direct bias current applied across the entire nano-pillar, as it is shown in Fig. 1(b), the perpendicular polarizers transfer the spin torque to the adjacent FLs, $\mathbf{T}_{S,\,i} \sim \mathbf{m}_i \times (\mathbf{m}_i \times \mathbf{p}_i)$, and this torque pushes the magnetizations of the FLs out of the (x, y) plane towards the opposite ends of the structure ($m_{z,\,\mathrm{b}} < 0$, $m_{z,\,\mathrm{t}} > 0$; $m_{z,\,i}$ is z-component of $\mathbf{m}_i$). The torque $\mathbf{T}_{D,\,i} \sim (\mathbf{m}_i \times (d\mathbf{m}_i/dt))$ created by Gilbert damping opposes this action of the spin torque and pushes the FL magnetizations back towards the plane of the device. The easy-plane demagnetizing fields arise in both FLs in proportion to their out of plane magnetization components ($\mathbf{B}_{d,\,i} \sim -m_{z,\,i}\,\hat{\mathbf{z}}$), and, as shown in Fig. 1(b), induce the FLs' magnetizations to undergo precession in opposite directions around the normal to the sample plane [34] in a zero bias dc magnetic field. This precession due to the GMR effect produces oscillations of the resistance of the whole nano-pillar, and the frequency of these oscillations is equal to the sum of the individual precession frequencies of the FLs. Thus, using the above described design of a DFL STNO it is possible to approximately double the generation frequency attainable with a single FL and fixed reference layer. The amplitude of the resistance oscillations in a DFL STNO is similar to the full amplitude of the GMR between the FLs, resulting in a relatively large microwave power emitted from the device [33].

B. A simplified model of a DFL STNO

Although the layout of a DFL STNO presented in Section II A contains four magnetic layers (two inner FLs and two outer PLs (see Fig. 1(a)) in the following we assume that the magnetizations of the PLs of the STNO are completely fixed and lie strictly perpendicular to the layers' plane, and, therefore, we consider only the STT-induced dynamics in the two FLs. We use the macrospin approximation to describe the magnetization dynamics in the FLs, i.e. we assume that each of the dimensionless vectors $\mathbf{m}_i = \mathbf{M}_i\,/M_{f,\,i}$ directed along the magnetization of the ith FL $\mathbf{M}_i$ depends only on time t for both FLs ($i = \{\mathrm{t},\,\mathrm{b}\}$). We also assume that the considered system operates in a zero bias dc magnetic field and is completely symmetric (the thicknesses and magnetic parameters of both FLs are the same. We consider a case when the FLs of the STNO are coupled with one another by a dipole-dipole interaction and are characterized by an easy-axis in-plane anisotropy, the magnitude of which will vary in our simulations.

Despite the obvious limitations of the chosen model it is sufficiently accurate in the case when the density J_{dc} of the bias dc current is lower ($J_{\mathrm{dc}} < J_{\mathrm{vortex}}$) than the density J_{vortex} corresponding to the vortex formation threshold calculated in [33]. We show below in Section III that our simplified numerical macrospin model of the DFL STNO allows one to correctly predict the value of the threshold J_{th} corresponding to the appearance of stable dynamics determined from the much more complicated and time-consuming micromagnetic simulations [33]. It also satisfactory describes the dependence of the generated microwave frequency on the density of the bias dc current J_{dc} for current densities below the threshold of vortex formation [33].

C. The equations for the magnetization dynamics in a DFL STNO

The dynamics of the normalized magnetization vectors $\mathbf{m}_i\,(t) = \mathbf{M}_i\,(t)/M_f$ in the ith FL ($i = \{\mathrm{t},\,\mathrm{b}\}$) under the action of a bias dc current with density J_{dc} is governed by the Landau-Lifshitz-Gilbert equation with an additional Slonczewski-Berger STT term describing the influence of a spin transfer torque [1, 2]:

$$\frac{d\mathbf{m}_i}{dt} = \mathbf{T}_{P,\,i} + \mathbf{T}_{D,\,i} + \mathbf{T}_{S,\,i}\,. \tag{1}$$

The first term, $\mathbf{T}_{P,\,i}$, in the right-hand side part of this equation describes the torque created by the effective magnetic field $\mathbf{B}_{\mathrm{eff},\,i}$ that causes the conservative precession of the unit vector $\mathbf{m}_i$ about the direction of this effective magnetic field [35]:

$$\mathbf{T}_{P,\,i} = \gamma\,[\mathbf{B}_{\mathrm{eff},\,i} \times \mathbf{m}_i]\ . \tag{2}$$

Here $\gamma = g\mu_{\mathrm{B}}/\hbar \approx 2\pi \cdot 28$ GHz/T is the modulus of the gyromagnetic ratio, g is the spectroscopic Lande factor, μ_{B} is the Bohr magneton, and $\hbar$ is the reduced Planck constant.

The second term, $\mathbf{T}_{D,\,i}$, is the dissipative Gilbert torque describing the energy dissipation, which can be written as [35]:

$$\mathbf{T}_{D,\,i} = \alpha\left[\mathbf{m}_i \times \frac{d\mathbf{m}_i}{dt}\right], \tag{3}$$

where α is the dimensionless Gilbert damping parameter of the FL (the same for both FLs).

The last term in the right-hand side part of Eq. (1), $\mathbf{T}_{S,\,i}$, is the Slonczewski-Berger STT term describing the interaction of the magnetization with the spin-polarized current traversing ith FL. The expression for this torque obtained in [1, 2] can be written as:

$$\mathbf{T}_{S,\,i} = -\sigma_i J_{\mathrm{dc},\,i}\,[\mathbf{m}_i \times (\mathbf{m}_i \times \mathbf{p}_i)]\ , \tag{4}$$

where $J_{\mathrm{dc},\,i}$ is the bias dc current density traversing the STNO (connected to the bias dc current $I_{\mathrm{dc},\,i}$ by the expression $I_{\mathrm{dc},\,i} = \pi R^2 J_{\mathrm{dc},\,i}$, where R is the radius of the nano-pillar), $\mathbf{p}_i$ is the unit vector along the magnetization of the PL ($\mathbf{p}_i = \hat{\mathbf{z}}$ in our simulations), and σ_i is the

"current density-spin torque" proportionality coefficient, which can be written in a general form as:

$$\sigma_i = \sigma_0 \varsigma(P, \beta_i)\,. \tag{5}$$

Here $\sigma_0 = (\gamma\hbar/2e)/(M_f L)$ is the angular-independent factor in the "current density-spin torque" coefficient σ_i, e is the modulus of the electron charge, M_f is the saturation magnetization of the FL, L is the thickness of the FL, and $\varsigma(P, \beta_i)$ is the factor describing the angular dependence of STT depending on the dimensionless degree P $(0 < P < 1)$ of the current spin-polarization and the angle β_i between the magnetizations of ith FL and its corresponding polarizer. The angular dependence $\varsigma(P, \beta_i)$ is different for the different spacer materials between the magnetic layers. In the case of a metallic spacer (considered in this work) this factor can be approximated by [1]:

$$\varsigma(P, \beta_i) = \left[\frac{(1+P)^3}{4P^{3/2}}(3 + \cos\beta_i) - 4\right]^{-1}, \tag{6}$$

where $\cos\beta_i = (\mathbf{m}_i \cdot \mathbf{p}_i)$. We specify the current density $J_{\mathrm{dc},\,i}$ in Eq. (4) as:

$$J_{\mathrm{dc},\,i} = \begin{cases} +J_{\mathrm{dc}}\,, & i = \mathrm{t}\ \text{(Top free layer)} \\ -J_{\mathrm{dc}}\,, & i = \mathrm{b}\ \text{(Bottom free layer)} \end{cases}, \tag{7}$$

with opposite signs in the two FLs due to the different order in which the spin-polarized electrons traverse the two polarizer/free-layer pairs.

In our model the effective magnetic field $\mathbf{B}_{\mathrm{eff},\,i}$ in Eq. (2) has the contributions from the self-demagnetization field $\mathbf{B}_{i,\,i}$, cross-demagnetization field $\mathbf{B}_{i,j}$ (the sum of these fields is the total demagnetization field acting on ith FL; i, j=$\{$t, b$\}$), and an easy-axis anisotropy field $\mathbf{B}_{\mathrm{A},\,i}$:

$$\mathbf{B}_{\mathrm{eff},\,i} = \mathbf{B}_{i,\,i} + \mathbf{B}_{i,j} + \mathbf{B}_{\mathrm{A},\,i}\,. \tag{8}$$

It is important to note, that the effective magnetic field $\mathbf{B}_{\mathrm{eff},\,i}$ does not include an external bias dc magnetic field, which stresses one more time the possibility of normal operation of a DFL STNO in a zero applied dc field.

The self-demagnetization field $\mathbf{B}_{i,\,i}$ and the cross-demagnetization field $\mathbf{B}_{i,j}$ are defined as follows [36]:

$$\mathbf{B}_{i,\,i} = -\mu_0 M_f \mathbf{N}_{i,\,i}\mathbf{m}_i\,, \tag{9a}$$

$$\mathbf{B}_{i,j} = -\mu_0 M_f \mathbf{N}_{i,j}\mathbf{m}_j\,, \tag{9b}$$

where μ_0 is the vacuum magnetic permeability, $\mathbf{N}_{i,\,i}$ is the self-demagnetization tensor

$$\mathbf{N}_{i,\,i} = \begin{pmatrix} \kappa & 0 & 0 \\ 0 & \kappa & 0 \\ 0 & 0 & 1-2\kappa \end{pmatrix}, \tag{10a}$$

and $\mathbf{N}_{i,j}$ is the cross-demagnetization tensor:

$$\mathbf{N}_{i,j} = \begin{pmatrix} \rho & 0 & 0 \\ 0 & \rho & 0 \\ 0 & 0 & -2\rho \end{pmatrix}. \tag{10b}$$

In Eqs. (10) we took into account the fact that the FLs have identical parameters, and, therefore, the dimensionless tensor elements κ and ρ depending on the geometry of the structure are the same for both the top and bottom FLs.

In the practically interesting case of thin magnetic layers, when the layers' thickness L and the thickness of the GMR spacer between the FLs d are substantially smaller than the radius of the structure R $(L, d \ll R)$, the tensor elements κ and ρ are given by the following expressions [36]:

$$\kappa = \frac{1}{2\pi}\frac{L}{R}\left[C - \ln\left(\frac{L}{R}\right)\right], \tag{11a}$$

$$\rho = \frac{C}{2\pi}\frac{L}{R} - \frac{1}{4\pi\,(L/R)}\left[F\left(\frac{d}{R}\right) - F\left(\frac{d+L}{R}\right) - F\left(\frac{d+L}{R}\right) + F\left(\frac{d+2L}{R}\right)\right], \tag{11b}$$

where $C = \ln(8) - 1/2$ and $F(\zeta) = \zeta^2 \ln|\zeta|$. Typically, κ and ρ are small quantities $(\kappa, \rho \ll 1)$. For instance, in the case of the DFL STNO with chosen typical parameters (see Section II D) $\kappa = 0.0707$, $\rho = 0.01134$.

An easy-axis anisotropy field of the ith FL was chosen to be directed along the x-axis, and is defined as [35]

$$\mathbf{B}_{\mathrm{A},\,i} = B_{\mathrm{A}}\,(\mathbf{m}_i \cdot \hat{\mathbf{x}})\,\hat{\mathbf{x}}\,, \tag{12}$$

where $B_{\mathrm{A}} > 0$ is the magnitude of the anisotropy field along the easy x-axis in both FLs.

The details about the numerical procedure of our macrospin simulations are presented in the Appendix (see Section V A for details).

D. Parameters of the DFL STNO

For a quantitative description of the DFL STNO's operation we used the following typical parameters of the nano-pillar structure [33]. We considered a symmetric circular nano-pillar with the radius $R = 25$ nm, 3 nm thick FLs ($L = L_{\mathrm{t}} = L_{\mathrm{b}} = 3$ nm) and 12 nm thick GMR spacers ($d = 12$ nm) (see Fig. 1(a)).

We assumed that both FLs have the saturation magnetization $M_f = M_{f,\mathrm{t}} = M_{f,\mathrm{b}} = 560$ emu/cm^3 (thus $\mu_0 M_f \approx 704$ mT), which is typical for thin Permalloy ($\mathrm{Ni}_{1-x}\mathrm{Fe}_x$) films sandwiched between the Cu layers [37].

We assumed a value of the current polarization to be $P = 0.3$, which is typical for GMR spin valves. It has been shown recently in [33] that the value of the Gilbert damping parameter, α, has a strong impact on the dynamics of a DFL STNO, and, therefore, we simulated the dynamic behavior of our model system in a wide range of α values 0.002-0.09 (the same for both FLs). The substantial increase of the FL damping can be realized in practice by doping the FL with Tb [38]. We also found that the magnetization dynamics in a DFL STNO significantly depends on the magnitude of the magnetic field

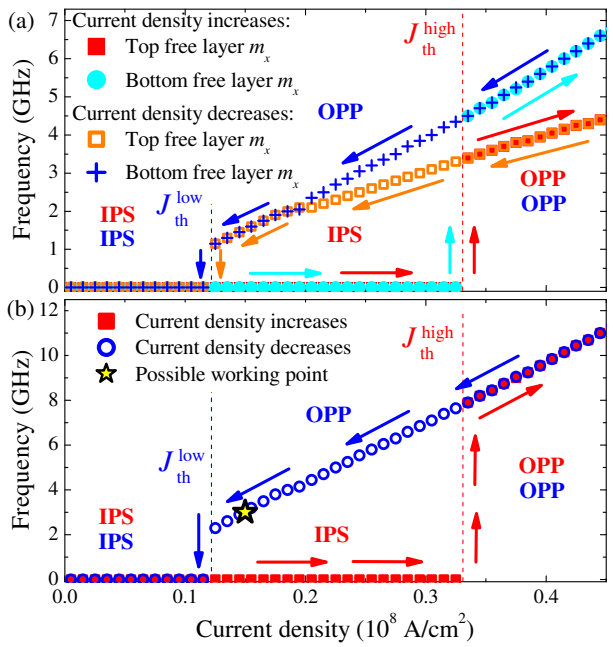

FIG. 2: (Color Online) (a) Numerically calculated dependences of the precession frequencies in the top $m_{x,\mathrm{t}}$ (f_t) and bottom $m_{x,\mathrm{b}}$ (f_b) FLs in a DFL STNO on the density J_dc of the bias dc current, demonstrating strong hysteresis. Dynamics starts at $J_\mathrm{dc} = J_\mathrm{th}^\mathrm{high}$ when the bias current increases (red squares and cyan circles) and stops at $J_\mathrm{dc} = J_\mathrm{th}^\mathrm{low}$ when the current decreases (orange hollow squares and blue crosses). The system can be in the in-plane static (IPS) or in the out-of-plane precessional (OPP) state. (b) Numerically calculated dependence of the frequency of an output signal f in a DFL STNO on the bias direct current density J_dc. The generated frequency is equal to the sum of the precession frequencies in the FLs, $f = f_\mathrm{t} + f_\mathrm{b}$. Yellow star marks a possible working point, which could be reached by using the procedure described in Section III C. The curves are calculated for $\alpha = 0.08$, $B_\mathrm{A} = 5$ mT. All the other parameters of the DFL STNO are presented in Section II D.

B_A of the easy-axis in-plane anisotropy (see Eq. (12)), and, therefore, performed simulations in which the field B_A (again, the same for both FLs) was varied in the range 0-20 mT.

III. RESULTS AND DISCUSSION

A. Hysteresis in the dependence of the generated frequency on the bias current

Using the macrospin simulation procedure, described in details in Section V A, we numerically solved the coupled Landau-Lifshitz-Gilbert equations with Slonczewski-Berger STT terms (1) for the magnetizations of the two FLs and calculated the frequencies of magnetization precession in the top and bottom FLs. The typical dependence of the frequency generated in a DFL STNO on the density J_dc of the applied bias dc current is shown in Fig. 2. As one can see, the frequency dependence on the bias current is different depending on whether the current density increases or decreases, i.e. this dependence demonstrates a strong hysteresis.

When the density of the dc bias current is increased (red squares and cyan circles in Fig. 2(a), red squares in Fig. 2(b)), the magnetizations in both FLs stay in plane (IPS) without any precession till the current density reaches a rather large magnitude $J_\mathrm{th}^\mathrm{high}$ ($J_\mathrm{th}^\mathrm{high} \approx 0.33{\cdot}10^8$ A/cm^2 in Fig. 2). Above this critical (threshold) value the magnetizations in both FLs start to precess in opposite directions, and the frequency of precession increases with the increase of the current density. Note, that the generated frequency just above the threshold has a rather large value (about 8 GHz, see Fig. 2(b)). However, when the density of the bias dc current is decreased (orange hollow squares and blue crosses in Fig. 2(a), blue hollow points in Fig. 2(b)), the regime of stable counter-precession of the FLs persists till rather low magnitudes of the bias current density $J_\mathrm{th}^\mathrm{low}$ ($J_\mathrm{th}^\mathrm{low} \approx 0.12 \cdot 10^8$ A/cm^2, (see Fig. 2), and the generated frequency which decreases with the decrease of current can be much lower (down to approximately 2 GHz).

Note, that the threshold value $J_\mathrm{th}^\mathrm{high}$ (at which the stable counter-precession in two FLs starts) obtained in our macrospin simulations is very close to the threshold value $J_\mathrm{th} \approx 0.35 \cdot 10^8$ A/cm^2 determined from the micromagnetic simulations [33]. This is a clear confirmation that our simplified "macrospin" model is sufficiently accurate to get even the quantitative information about the characteristics of DFL STNO. One can also note, that the difference between the frequencies of magnetization precession in the top and bottom layer of the DFL STNO (f_t and f_b, respectively) is caused by the angular dependence of the STT given by Eq. (6). If in our simulations we assume that $\cos\beta_i = \mathrm{const}$ in Eq. (6), the hysteresis behavior of the DFL STNO remains the same as before, but the precession frequencies of the top and bottom layers f_t and f_b become equal.

The origin of the hysteresis in DFL STNO may be qualitatively explained as follows. In the absence of a bias dc current the system exists in the so-called "in-plane state" (IPS). In this state the magnetizations of the FLs are dipolarly coupled to each other and the energy of the system is minimal when the magnetizations have opposite directions. In other words, the dipolar coupling creates a potential well for the magnetizations (the in-plane anisotropy has a similar effect), and a finite torque (and, therefore, a finite bias current density $J_\mathrm{th}^\mathrm{high}$) is required to move the magnetizations out of this potential well. Thus, the higher threshold current $J_\mathrm{th}^\mathrm{high}$ is determined by the depth of this potential well and depends, mainly, on the strengths of the dipolar coupling between the FLs and/or on the strength of the in-plane anisotropy field. However, once the dipolar coupling between the two FLs is destroyed by a sufficiently strong spin torque created by the bias current, a much smaller spin torque is suffi-

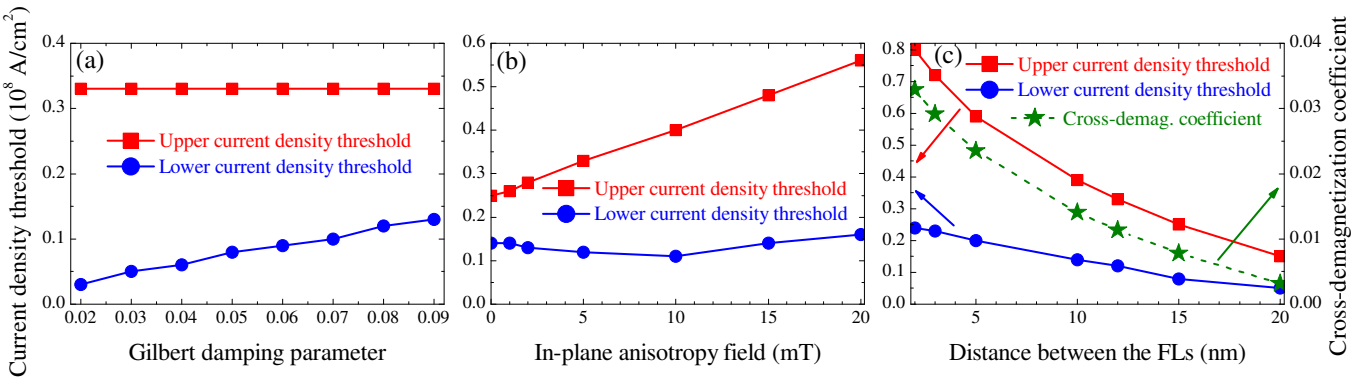

FIG. 3: (Color Online) Numerically calculated dependences of the current density thresholds $J_{\rm th}^{\rm low}$ (blue circles and line) and $J_{\rm th}^{\rm high}$ (red squares and line) on the different parameters of the DFL STNO. (a) The dependence of $J_{\rm th}^{\rm low}$ and $J_{\rm th}^{\rm high}$ on the Gilbert damping parameter α. (b) The dependence of $J_{\rm th}^{\rm low}$ and $J_{\rm th}^{\rm high}$ on the magnitude of the in-plane anisotropy field $B_{\rm A}$. (c) The dependence of $J_{\rm th}^{\rm low}$ and $J_{\rm th}^{\rm high}$ on the distance between the FLs d. Green stars and dashed line show the dependence of the cross-demagnetization coefficient ρ on d, $\rho(d)$. All the curves are calculated for $\alpha = 0.08$, $B_{\rm A} = 5$ mT (if other values of parameters are not mentioned specifically). All the other parameters of the DFL STNO are presented in Section II D.

cient to sustain the persistent magnetization precession: as in the other types of STNO, the spin torque only needs to compensate the natural Gilbert damping in the FLs. Thus, the lower critical current $J_{\rm th}^{\rm low}$ is determined by the energy losses and should be approximately proportional to the Gilbert damping constant α.

B. Threshold bias current densities of the DFL STNO

To verify the above described qualitative picture, we performed detailed investigations of the dependence of the critical current densities $J_{\rm th}^{\rm high}$ and $J_{\rm th}^{\rm low}$ on various system parameters. In accordance with the above presented explanations, the critical currents in DFL STNO should depend on three major factors: (a) Gilbert damping parameter α of the system, (b) easy-axis anisotropy field with magnitude $B_{\rm A}$, and (c) dipolar coupling between the FLs, dependent on the system geometric parameters (e.g the distance d between the FLs) and characterized by the cross-demagnetization coefficient $\rho(d)$. The numerically calculated dependences of both critical currents on these parameters are presented in Fig. 3.

One can see from Fig. 3(a), that the upper threshold $J_{\rm th}^{\rm high}$ (red squares and line) does not depend on the damping parameter α, while the lower threshold $J_{\rm th}^{\rm low}$ (blue circles with line) increases linearly with α. The dependence $J_{\rm th}^{\rm low}(\alpha)$ is similar to a similar relation for a conventional single-free-layer STNO, where the magnetization of a FL can precess relative "freely", when an applied bias current compensates the natural damping in the system. In that case in a conventional STNO there is a linear relation between the threshold current and the Gilbert damping parameter α and a similar dependence $J_{\rm th}^{\rm low}(\alpha)$ is seen in our DFL STNO.

At the same time, the fact that the higher threshold $J_{\rm th}^{\rm high}$ is independent of damping shows that the origin of this upper threshold current is non-dissipative. In contrast the curve of a linear dependence of $J_{\rm th}^{\rm high}$ on the magnitude of the in-plane anisotropy field $B_{\rm A}$ (red squares and line), shown in Fig. 3(b), indicates that a strong in-plane anisotropy field acts in the same manner as a dipolar coupling between the FLs: it prevents the appearance of a stable magnetization precession and creates a finite dc current density threshold for this precession which increases linearly with the increase of the anisotropy field. In contrast to the clear linear dependence $J_{\rm th}^{\rm high}(B_{\rm A})$, the dependence of the low current density threshold $J_{\rm th}^{\rm low}$ on $B_{\rm A}$ (blue circles and line, see Fig. 3(b)) is relatively weak.

The other interesting result is that the above described hysteresis exists even in the absence of an in-plane anisotropy field. In that case its existence is determined by the dipolar coupling between the FLs only. The curves $J_{\rm th}^{\rm high}(d)$ (red squares and line), $J_{\rm th}^{\rm low}(d)$ (blue circles and line), and $\rho(d)$ (green stars and line) calculated for different values of the distance between the FLs d are presented in Fig. 3(c) These curves convincingly show a substantial effect of the dipolar coupling between the FLs on the magnetization dynamics in the DFL STNO.

Comparing the curves $J_{\rm th}^{\rm high}(d)$ and $\rho(d)$ it becomes obvious, that the upper current density threshold is proportional to the cross-demagnetization coefficient of the system ρ, $J_{\rm th}^{\rm high} \sim \rho$. This means that the upper current density threshold $J_{\rm th}^{\rm high}$ can be selected by choosing an appropriate geometry of the system giving some particular value of the parameter ρ. Although the low current density threshold $J_{\rm th}^{\rm low}$ also depends on ρ, this dependence is substantially weaker in comparison to the dependence of the upper current density threshold. Consequently, one can easily change the width of the hysteresis loop defined

as $(J_{\rm th}^{\rm high} - J_{\rm th}^{\rm low})$ by choosing a particular value of the geometric factor ρ dependent on the thickness L and radius R of the FLs and on the distance d between the FLs (see Eq. (11b) for details).

C. Stable magnetization dynamics in a DFL STNO for bias current densities below the upper threshold

The discovered hysteretic behavior of the DFL STNO implies the possibility of application of a strong initial pulse of the bias current (greater than the upper threshold of the stable dynamics $J_{\rm th}^{\rm high}$) and subsequent reduction of the bias current to a working point corresponding to the required output frequency. In order to prove this statement we performed a numerical experiment when the STNO is biased by a dc current density $J_{\rm dc}(t) = J_{\rm dc}^{\rm work} + J_{\rm dc}^{\rm pulse}(t)$.

The supplied bias current signal consists of two independent component: a constant "working" dc current with density $J_{\rm dc}^{\rm work} = 0.15 \cdot 10^8$ A/cm^2, that is substantially smaller than the upper threshold of the stable dynamics $J_{\rm th}^{\rm high}$ (the working point corresponding to the $J_{\rm dc}^{\rm work}$ is shown by the yellow star in Fig. 2), and an initial pulse of the bias current characterized by a current density $J_{\rm dc}^{\rm pulse}(t)$ and duration $T_{\rm pulse}$.

In the numerical experiment we studied how the magnetizations of the FLs, characterized by the unit vectors $\mathbf{m}_{\rm t}(t)$, $\mathbf{m}_{\rm b}(t)$, evolve from the initial equilibrium anti-parallel configuration $[\mathbf{m}_{\rm t}(0) = (1,0,0)$, $\mathbf{m}_{\rm b}(0) = (-1,0,0)]$ over time t, when the bias current density $J_{\rm dc}(t)$ passes through the DFL STNO. We considered three different cases: when the bias current density is constant ($J_{\rm dc}^{\rm pulse} = 0$, Fig. 4(a)), when the rectangular pulse of the bias current has magnitude of $J_{\rm dc}^{\rm pulse} = 0.1 \cdot 10^8$ A/cm^2 not exceeding the higher threshold of the magnetization dynamics (Fig. 4(b)), and the third case when $J_{\rm dc}^{\rm pulse} = 0.2 \cdot 10^8$ A/cm^2 is over the higher threshold of the magnetization dynamics (Fig. 4(c)). The pulse duration in the last two cases was $T_{\rm pulse}$= 0.5 ns.

It can be seen from Fig. 4 that the dynamics of the system, described by the time profiles of the in-plane $m_{x,{\rm t}}\,(t)$ (blue curve) and out-of-plane $m_{z,{\rm t}}\,(t)$ (red curve) components of the unit vector $\mathbf{m}_{\rm t}\,(t)$ in the top FL [39] of the DFL STNO, critically depends on the amplitude $J_{\rm dc}^{\rm pulse}$ of the pulsed component of the bias current. A weak constant dc current density $J_{\rm dc}^{\rm work}$ induces only small perturbations of the IPS stationary state of the DFL STNO (see Fig. 4(a)). When the initial pulse is present in the bias current, but the total initial amplitude of the current density $J_{\rm dc}^{\rm work} + J_{\rm dc}^{\rm pulse}$ does not exceed the higher threshold of the magnetization dynamics in the DFL STNO, such a pulse creates a transient dynamical process, but the IPS state of the system remains stable after the end of the current pulse (see Fig. 4(b)). The situation changes dramatically when a strong initial pulse of the bias ($J_{\rm dc}^{\rm pulse} = 0.2 \cdot 10^8$ A/cm^2) is applied. If the total initial amplitude of the current density $J_{\rm dc}^{\rm work} + J_{\rm dc}^{\rm pulse}$ exceeds the higher threshold $J_{\rm th}^{\rm high}$ of the stable magnetization dynamics in the DFL STNO the stable magnetization precession is excited in both FLs of the DFL STNO, and this dynamics persists after the end of the initial current pulse (see Fig. 4(c) for the magnetization dynamics in the top FL).

The obtained results clearly show that it is possible to achieve a regime of stable counter-precession of FLs in the DFL STNO for relatively low bias dc current densities (below the the higher threshold of the DFL STNO stable dynamic) if a short pulse of bias current exceeding this threshold is applied initially.

IV. SUMMARY

In conclusion, we report that in a DFL STNO operating in the absence of a bias dc magnetic field there is a strong hysteresis in the dependence of the frequency generated by the STNO on the bias dc current. When the bias current is increased the microwave dynamics in the DFL STNO starts at a relatively high value of a bias current density, but when the bias current is decreased this dynamics persists till a much lower value of the bias current density. The lower threshold current is determined by the Gilbert damping parameter (precessional state vanishes due to the damping), while the higher threshold in the bias current is mainly caused by the existence of the in-plane anisotropy and dipolar coupling between the FLs. The discovered hysteretic behavior of a DFL STNO implies the possibility of application of a sufficiently strong initial pulse of the bias current (larger than the higher threshold of the stable magnetization dynamics) and subsequent reduction of the bias current to a working point corresponding to the required generated frequency. We believe the obtained results will be important for the practical development of DFL STNOs with optimized working characteristics.

ACKNOWLEDGEMENTS

This work was supported in part by the Contract from the U.S. Army TARDEC, RDECOM, by the Grants No. ECCS-1001815, ECCS-1002358, DMR-1015175 and DMR-0748810 from the National Science Foundation of the USA, by the CNFD grant from the "Semiconductor Research Corporation", by the Nanoelectronics Research Initiative through the Western Institute of Nanoelectronics, by the DARPA MTO/MESO grant N66001-11-1-4114, and by the Grant No. UU34/008 from the State Fund for Fundamental Research of Ukraine.

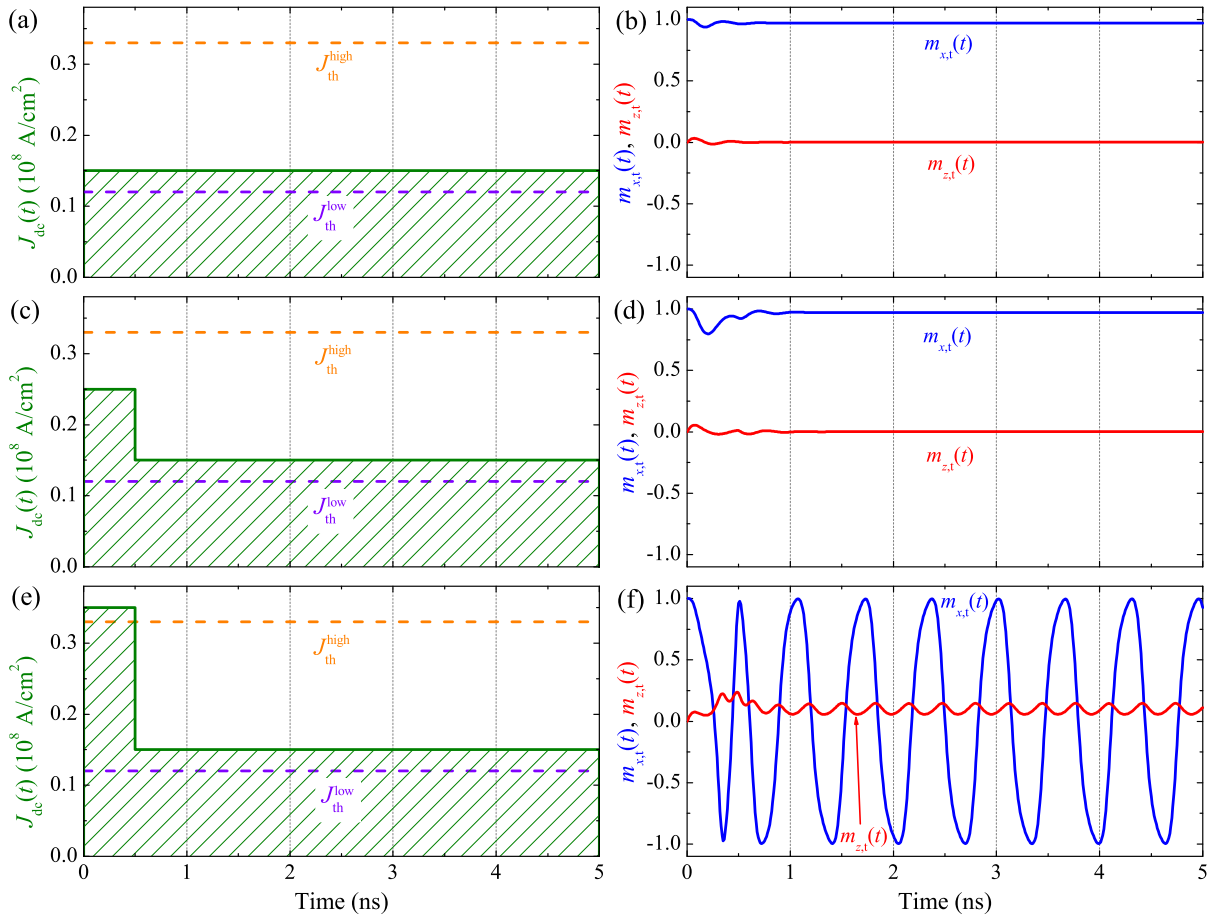

FIG. 4: (Color Online) Numerically calculated time profiles of the in-plane ($m_{x,\mathrm{t}}(t)$, blue curve) and out-of-plane ($m_{z,\mathrm{t}}(t)$, red curve) magnetization components in the top FL of the DFL STNO for different regimes of time-dependent current biasing (b, d, f). The DFL STNO is biased by a dc current density having a constant and a pulsed components $J_{\mathrm{dc}}(t) = J_{\mathrm{dc}}^{\mathrm{work}} + J_{\mathrm{dc}}^{\mathrm{pulse}}(t)$ and its time profile is shown by the green curve with green shading (a, c, e). Dashed horizontal lines show the levels corresponding to the higher (orange lines) and lower (violet lines) current thresholds ($J_{\mathrm{th}}^{\mathrm{high}}, J_{\mathrm{th}}^{\mathrm{low}}$). (a) The constant current density below the higher threshold $J_{\mathrm{dc}}^{\mathrm{work}} = 0.15 \cdot 10^8$ A/cm^2 induces only small perturbations of the IPS magnetization state (b). (c) The current density containing a constant part and a pulse of the duration 0.5 ns with the amplitude $J_{\mathrm{dc}}^{\mathrm{pulse}} = 0.1 \cdot 10^8$ A/cm^2 (still below the higher threshold) induces some transient dynamics, but in the end the IPS magnetization state remains stable (d). (e) The current density containing a constant part (above the lower threshold) and a strong pulse of the duration T_{pulse}=0.5 ns with the amplitude $J_{\mathrm{dc}}^{\mathrm{pulse}} = 0.2 \cdot 10^8$ A/cm^2 (exceeding the higher threshold) induces a stable magnetization precession (f). The curves are calculated for $\alpha = 0.08$, $B_{\mathrm{A}} = 5$ mT. All other parameters of the DFL STNO are presented in Section II D.

V. APPENDIX

A. Simulation procedure

Our macrospin simulations were based on the numerical solution of a pair of coupled Landau-Lifshits-Gilbert-Slonczewski (LLGS) equations (1) for both top and bottom FLs biased by a dc current density (7), where the effective magnetic field is given by Eq. (8) and the spin torque term is given by Eq. (5).

In order to explore the spectrum of a microwave signal generated by the DFL STNO under the action of a bias dc current, we assumed the current density J_{dc} to be a slow variable $J_{\mathrm{dc}}(t)$, that changes with time linearly at a sufficiently slow rate:

$$J_{\mathrm{dc}}(t) = \begin{cases} \eta t\,, & 0 \le t \le \dfrac{T_{\mathrm{sim}}}{2} \\ J_{\mathrm{dc}}^{\max} - \eta\left(t - \dfrac{T_{\mathrm{sim}}}{2}\right), & \dfrac{T_{\mathrm{sim}}}{2} \le t \le T_{\mathrm{sim}} \end{cases}, \tag{13}$$

where $\eta = |dJ_{\mathrm{dc}}(t)/dt|$ is the time rate of the current density variation, $J_{\mathrm{dc}}^{\max} = 0.5\eta T_{\mathrm{sim}}$ is the maximum density of the bias dc current traversing the DFL STNO and T_{sim} is the total simulation time. During the first half of that time, $0 \le t \le 0.5T_{\mathrm{sim}}$, the current density increases, while during the second half of that time, $0.5T_{\mathrm{sim}} \le t \le T_{\mathrm{sim}}$, it decreases. We performed a series of simulations with different values of η and found that

the chosen value of η, $\eta = 5 \cdot 10^7$ A/(cm$^2 \mu$s), does not noticeably perturb the magnetization dynamics, so that the variations of the current density (13) can be considered as quasi-static.

While solving the coupled LLGS equations (1) we used the following initial conditions for the unit vectors at $t = 0$: $\mathbf{m}_\mathrm{t}(0) = (1, 0, 0)$, $\mathbf{m}_\mathrm{b}(0) = (-1, 0, 0)$. As a result of a numerical solution we obtained the time profiles of the unit vectors $\mathbf{m}_\mathrm{t} \equiv \mathbf{m}_\mathrm{t}(t)$ and $\mathbf{m}_\mathrm{b} \equiv \mathbf{m}_\mathrm{b}(t)$ in the range of time $0 \le t \le T_\mathrm{sim}$ in top and bottom FLs, respectively. Using the discrete Fourier transform procedure for the x-components of the calculated profiles, $m_{x,\mathrm{t}}(t)$ and $m_{x,\mathrm{b}}(t)$, we calculated the frequencies of the magnetization oscillations in the top and bottom FLs, f_t and f_b, respectively. The characteristic accuracy of the calculated frequencies in our simulations was about 50 MHz , which was sufficient for the quantitative comparison of our results with the results of micromagnetic simulations and possible laboratory experiments.

When analyzing the possibility to excite a stable magnetization dynamics in the FLs for bias dc current densities J_dc lower than the upper threshold $J_\mathrm{th}^\mathrm{high}$, we assumed that the DFL STNO is biased by the dc current density consisting of two components. The first one was an initial current pulse of the density magnitude $J_\mathrm{dc}^\mathrm{pulse}$ and duration T_pulse, while the second one was a constant current density $J_\mathrm{dc}^\mathrm{work}$ which determined the required output frequency of a microwave signal generated by the DFL STNO:

$$J_\mathrm{dc}(t) = \begin{cases} J_\mathrm{dc}^\mathrm{work} + J_\mathrm{dc}^\mathrm{pulse}, & 0 \le t \le T_\mathrm{pulse} \\ J_\mathrm{dc}^\mathrm{work}, & T_\mathrm{pulse} \le t \le T_\mathrm{sim} \end{cases} . \quad (14)$$

[1] J. C. Slonczewski, J. Magn. Magn. Mat. **159**, L1 (1996).
[2] L. Berger, Phys. Rev. B **54**, 9353 (1996).
[3] M. D. Stiles and A. Zangwill, Phys. Rev. B **66**, 014407 (2002).
[4] D. C. Ralph and M. D. Stiles, J. Magn. Magn. Mater. **320**, 1190 (2008).
[5] A. Slavin and V. Tiberkevich, IEEE Trans. Magn. **45**, 1875 (2009).
[6] E. Y. Tsymbal, I. Žutić (Eds.), *Handbook of Spin Transport and Magnetism* (CRC Press, New York, 2012).
[7] S. I. Kiselev, J. C. Sankey, I. N. Krivorotov, N. C. Emley, R. J. Schoelkopf, R. A. Buhrman, and D. C. Ralph, Nature (London) **425**, 380 (2003).
[8] K. J. Lee, A. Deac, O. Redon, J.-P. Nozières, and B. Dieny, Nature Mater. **3**, 877 (2004).
[9] S. Kaka, M. R. Pufall, W. H. Rippard, T. J. Silva, S. E. Russek, and J. A. Katine, Nature (London) **437**, 389 (2005).
[10] F. B. Mancoff, N. D. Rizzo, B. N. Engel, and S. Tehrani, Nature (London) **437**, 393 (2005).
[11] I. N. Krivorotov, N. C. Emley, J. C. Sankey, S. I. Kiselev, D. C. Ralph, and R. A. Buhrman, Science **307**, 228 (2005).
[12] O. Boulle, V. Cros, J. Grollier, L. G. Pereira, C. Deranlot, F. Petroff, G. Faini, J. Barnaś, and A. Fert, Nature Phys. **3**, 492 (2007).
[13] V. S. Pribiag, I. N. Krivorotov, G. D. Fuchs, P. M. Braganca, O. Ozatay, J. C. Sankey, D. C. Ralph, and R. A. Buhrman, Nature Phys. **3**, 498 (2007).
[14] A. M. Deac, A. Fukushima, H. Kubota, H. Maehara, Y. Suzuki, S. Yuasa, Y. Nagamine, K. Tsunekawa, D. D. Djayaprawira, and N. Watanabe, Nature Phys. **4**, 803 (2008).
[15] A. Ruotolo, V. Cros, B. Georges, A. Dussaux, J. Grollier, C. Deranlot, R. Guillemet, K. Bouzehouane, S. Fusil, and A. Fert, Nature Nanotech. **4**, 528 (2009).
[16] V. E. Demidov, S. Urazhdin, and S. O. Demokritov, Nature Mater. **9**, 984 (2010).
[17] O. Prokopenko, E. Bankowski, T. Meitzler, V. Tiberkevich, and A. Slavin, IEEE Magn. Lett. **2**, 3000104 (2011).
[18] A. A. Tulapurkar, Y. Suzuki, A. Fukushima, H. Kubota, H. Maehara, K. Tsunekawa, D. D. Djayaprawira, N. Watanabe, and S. Yuasa, Nature (London) **438**, 339 (2005).
[19] Y. Suzuki, and H. Kubota, J. Phys. Soc. Jpn. **77**, 031002 (2008).
[20] C. Wang, Y.-T. Cui, J. Z. Sun, J. A. Katine, R. A. Buhrman, and D. C. Ralph, J. Appl. Phys. **106**, 053905 (2009).
[21] S. Ishibashi, T. Seki, T. Nozaki, H. Kubota, S. Yakata, A. Fukushima, S. Yuasa, H. Maehara, K. Tsunekawa, D. D. Djayaprawira, and Y. Suzuki, Appl. Phys. Express **3**, 073001 (2010).
[22] X. Cheng, C. T. Boone, J. Zhu, and I. N. Krivorotov, Phys. Rev. Lett. **105**, 047202 (2010).
[23] O. Prokopenko, G. Melkov, E. Bankowski, T. Meitzler, V. Tiberkevich, and A. Slavin, Appl. Phys. Lett. **99**, 032507 (2011).
[24] O. V. Prokopenko, I. N. Krivorotov, E. Bankowski, T. Meitzler, S. Jaroch, V. S. Tiberkevich, and A. N. Slavin, J. Appl. Phys. **111**, 123904 (2012).
[25] O. V. Prokopenko, I. N. Krivorotov, T. J. Meitzler, E. Bankowski, V. S. Tiberkevich, and A. N. Slavin, *Spin-Torque Microwave Detectors*, in book: S. O. Demokritov, and A. N. Slavin (Eds.), *Magnonics: From Fundamentals to Applications* (Topics in Applied Physics, Vol. 125) (Springer-Verlag, Berlin, 2013).
[26] J. A. Katine and E. E. Fullerton, J. Magn. Magn. Mater. **320**, 1217 (2008).
[27] P. M. Braganca, B. A. Gurney, B. A. Wilson, J. A. Katine, S. Maat, and J. R. Childress, Nanotechnology **21**, 235202 (2010).
[28] D. Houssameddine, U. Ebels, B. Delaët, B. Rodmacq, I. Firastrau, F. Ponthenier, M. Brunet, C. Thirion, J.-P. Michel, L. Prejbeanu-Buda, M.-C. Cyrille, O. Redon, and B. Dieny, Nature Mater. **6**, 447 (2007).
[29] I. Firastrau, D. Gusakova, D. Houssameddine, U. Ebels, M.-C. Cyrille, B. Delaët, B. Dieny, O. Redon, J.-C. Toussaint, and L. D. Buda-Prejbeanu, Phys. Rev. B **78**, 024437 (2008).
[30] U. Ebels, D. Houssameddine, I. Firastrau, D. Gusakova, C. Thirion, B. Dieny, and L. D. Buda-Prejbeanu, Phys. Rev. B **78**, 024436 (2008).
[31] G. Rowlands, I. Krivorotov, Abstracts of the 2009 APS

March Meeting, BAPS.2009.MAR.W29.7, Pittsburgh, PA, 2009.
[32] T. Moriyama, G. Finocchio, M. Carpentieri, B. Azzerboni, D. C. Ralph, and R. A. Buhrman, Phys. Rev. B **86**, 060411(R) (2012).
[33] G. E. Rowlands, and I. N. Krivorotov, Phys. Rev. B **86**, 094425 (2012).
[34] A. D. Kent, B. Özyilmaz, and E. del Barco, Appl. Phys. Lett. **84**, 3897 (2004).
[35] A. G. Gurevich and G. A. Melkov, *Magnetization Oscillations and Waves* (CRC: New York, 1996).
[36] O. Dmytriiev, T. Meitzler, E. Bankowski, A. Slavin and V. Tiberkevich, J. Phys.: Condens. Matter, **22**, 136001 (2010).
[37] C. Boone, J. A. Katine, J. R. Childress, J. Zhu, X. Cheng, and I. N. Krivorotov, Phys. Rev. B **79**, 140404(R) (2009).
[38] W. Bailey, P. Kabos, F. Mancoff, and S. E. Russek, IEEE T. Magn. **37**, 1749 (2001).
[39] The magnetization of the bottom FL of the DFL STNO exhibits very similar dynamics to the magnetization dynamics of the top FL and, therefore, time profiles $m_{x,\mathrm{b}}(t)$ and $m_{z,\mathrm{b}}(t)$ are not shown in this article.